Partonic Picture of Nuclear Shadowing at Small x

(*Ina Sarcevic, Zheng Huang and Hung Jung Lu*)

The theoretical studies of semihard processes play a increasingly important role in ultrarelativistic heavy-ion collisions at $\sqrt{s} \geq 200$ GeV in describing the global collision features such as particle multiplicities and transverse energy distributions. These semihard processes can be reliably calculated in the framework of perturbative QCD and they are crucial for determining the initial condition for the possible formation of a quark-gluon plasma. Assuming the validity of the factorization theorem in perturbation theory, it is essential to know the parton distributions in nuclei in order to compute these processes. For example, to calculate the minijet production for $p_T \sim 2$ GeV or the charm quark production in the central rapidity region ($y = 0$), one needs to know the nuclear gluon structure function $xg_A(x, Q^2)$ at $Q \sim p_T$ or m_c and $x = x_{\rm Bj} = 2p_T/\sqrt{s}$ or $2m_c/\sqrt{s}$. For $\sqrt{s} \geq 200$ GeV, the corresponding value of x is $x \leq 10^{-2}$. Similarly, the nuclear quark density $xf_A(x, Q^2)$ is needed for the Drell-Yan lepton-pair production process.

The attenuation of quark density in a nucleus has been firmly established experimentally at CERN [1] and Fermilab [2] in the region of small values of the Bjorken variable $x = Q^2/2m\nu$ in deeply-inelastic lepton scatterings (DIS) off nuclei, where Q^2 is the four-momentum transfer squared, ν is the energy loss of the lepton and m is the nucleon mass. The data, taken over a wide kinematic range, $10^{-5} < x < 0.1$ and 0.05 GeV$^2 < Q^2 < 100$ GeV^2, show a systematic reduction of nuclear structure function $F_2^A(x, Q^2)/A$ with respect to the free nucleon structure function $F_2^N(x, Q^2)$. There are also some indications of nuclear gluon shadowing from the analysis of J/Ψ suppression in hadron-nucleus experiments [3]. Unfortunately, the extraction of nuclear gluon density is not unambiguous since it involves the evaluation of the initial parton energy loss and final state interactions [4].

The partonic description of nuclear shadowing phenomenon has been extensively investigated in literatures in the context of a recombination model [5, 6, 7] and in a Glauber multiple scattering theory [8, 9, 10, 11, 12]. These approaches predict different scale (Q^2) dependence of the nuclear structure function than the conventional Gribov-Lipatov-Altarelli-Parisi (GLAP) evolution equation [13]. Qualitatively, the scale evolution of the nuclear structure function is slower than the nucleon case, leading to a perturbative mechanism for the depletion of the parton density at large momentum transfer. The quantitative prediction of nuclear shadowing at large Q^2 in general depends on the initial value of shadowing at a small momentum transfer where a perturbative calculation breaks down and some non-perturbative model or experimental input is needed. The so-called vector-meson-dominance (VMD) model [14] has been quite successful in predicting the quark shadowing at small Q^2 where the experimental data is rich [1, 2]. Presently there is no viable non-perturbative model for the gluon case and there is very little experimental information on the initial gluon shadowing value at some small Q_0^2. This, in principle, could make the prediction on gluon shadowing very uncertain.

We suggest that these exists a typical scale $Q_{\rm SH}^2 \simeq 3$ GeV^2 in the perturbative evolution of the nuclear gluon density beyond which the nuclear gluon shadowing can be unambiguously predicted in the context of perturbative QCD [15]. The so-called "semihard" scale $Q_{\rm SH}^2$

is determined by the strength of the scaling violation of the nucleon gluon density in the small-x region at which the anomalous dimension $\gamma \equiv \partial \ln xg_N / \ln Q^2$ is of $O(1)$. We demonstrate that as Q^2 approaches $Q^2_{\rm SH}$, the gluon shadowing ratio rapidly approaches a unique perturbative value determined by the Glauber multiple scattering theory. At $Q^2 > Q^2_{\rm SH}$, the nuclear gluon density, in contrast to the quark case, is almost independent of the initial distribution at Q_0^2 and its evolution is mainly governed by a GLAP equation. The suggested phenomenon is intimately related to the singular growth of the gluon density in the small-x region and the perturbative shadowing caused by the coherent parton multiple scattering.

We have studied the x-dependence of the shadowing ratio and the non-saturating feature of the perturbative shadowing. As a by-product of the Glauber approach, we have also considered the nuclear geometry dependence of the shadowing ratio, which cannot be addressed in the recombination model such as the GLR equation. Since the shadowing effect is intimately related to the effective number of scatterings, it should vary strongly as one changes the impact parameter. This leads to the breakdown of the conventional factorization of the nuclear parton density into the product of an impact parameter averaged parton distribution and the nuclear thickness function.

At low Q^2, $Q^2 < 1$ GeV^2, in the deeply-inelastic scattering, the interaction of the virtual photon with the nucleons in the rest frame of the target is most naturally described by a vector-meson-dominance (VMD) model [14], in which the virtual photon interacts with the nucleons via its hadronic fluctuations, namely the ρ, ω and ϕ mesons. The shadowing of the (sea) quark density is caused by the coherent multiple scatterings of the vector meson off the nucleons with a large hadronic cross section σ_{VN}, which can be most conveniently handled by the Glauber diffractive approximation model [16]. The x-dependence of the shadowing ratio $R(x, Q^2) = F_2^A(x, Q^2)/AF_2^N(x, Q^2)$ is explained by the coherent length of the virtual photon $l_c \simeq 1/2mx$. For $x < 10^{-2}$, $l_c > R_A = 4 \sim 5$ fm for large nuclei, the vector meson interacts coherently all nucleons inside the nucleus resulting in a uniform (in x) reduction of the total cross section, while for $x > 10^{-2}$, $l_c < R_A$ the vector meson can only interact coherently with a fraction of all the nucleons and shadowing is reduced. However, the VMD model in general predicts much less scaling violation of $F_2^N(x, Q^2)$ than it is observed in the small x region and a rapid disappearance of the nuclear shadowing as $Q^2 \gg m_V^2$. Although a generalized VMD model which includes higher resonances may improve the situation somewhat, it is generally believed that the nuclear shadowing in the VMD model is a higher twist effect, which is in contraction with the experimental evidence that the $R(x, Q^2)$ has a rather weak Q^2 dependence [1, 2].

At $Q^2 > 1 \sim 2$ GeV^2, the virtual photon can penetrate the nucleon and probe the partonic degrees of freedom where a partonic interpretation based on perturbative QCD is most relevant in the infinite momentum frame. It is well known that the Q^2-dependence, the so-called scaling violation of the nucleon structure function $F_2^N(x, Q^2)$ can be well accounted for by the GLAP evolution equation given some non-perturbative initial condition $F_2^N(x, Q_0^2)$ [17]. In the small x region, the GLAP predicts a strong scaling violation of $F_2^N(x, Q^2)$ due to the strong growth of the gluon density in the nucleon. In fact, a dominant perturbative evolution implies that the growth of $F_2^N(x, Q^2)$ in $\ln Q^2$ at fixed, small x is closely related to the growth in $\ln 1/x$ at fixed Q^2, i.e. the so-called double scaling violation observed in the DIS experiments for nucleon, most transparent in the Double Leading-Logarithm Approximation (DLA) of the gluon structure function. At extremely small x, the resummation of large $\ln 1/x$ is necessary leading to the BFKL evolution equation [18] which may also be derived in a Weiszacker-Williams classical field approximation [19]. It is not clear when the BFKL hard pomeron will become relevant since the GLAP evolution seems able to describe most of kinematical region that current experiments have probed so far. As we show, the main feature of the Q^2-dependence of the nuclear shadowing is intimately related to this strong scaling violation in the small-x region. In the target rest frame, the virtual photon interacts with nucleons via its quark-antiquark pair ($q\bar{q}$) color-singlet fluctuation [9]. If the coherence length of the virtual photon is larger than the radius of the nucleus, $l_c > R_A$, the $q\bar{q}$ configuration interacts coherently with all nucleon with a cross section given by the color transparency mechanism for a point-like color-singlet configuration [20]. That is, the cross section is proportional to the transverse separation squared, r_t^2, of the q and $\bar{q}$. In the double logarithm approximation (DLA), the cross section can be expressed through the gluon structure function for a nucleon [21]

$$\sigma_{q\bar{q}N} = \frac{4\pi^2}{3} r_t^2 \alpha_s x' g_{\rm DLA}(x', 1/r_t^2) \ , \tag{1}$$

where $x' = M^2/2m\nu$ and M is the invariant mass of $q\bar{q}$ pair.

The Glauber multiple-scattering theory [16] treats nuclear collision as a succession of collisions of the probe with individual nucleons within nucleus. A partonic system (h), being a $q\bar{q}$ or a gg fluctuation, can scatter coherently from several or all nucleons during its passage through the target nucleus. The interference between the multiple scattering amplitudes causes a reduction of the hA cross section compared to the naive scaling result of A times the respective hN cross section, the origin of the nuclear shadowing. In the high-energy eikonal limit, the phase shift of the elastic hA scattering amplitude is just the sum of the individual hN scatterings. The total hA cross section is determined by the imaginary part of the forward elastic scattering amplitude as governed by the unitarity relation or the optical theorem. The unitarity of the total cross section is thus built-in within the Glauber theory.

The total hA cross section is given by

$$\sigma_{hA} = \int d^2\mathbf{b} 2 \left[1 - e^{-\sigma_{hN} T_A(\mathbf{b})/2}\right] \ . \tag{2}$$

For a Gaussian parametrization of $T_A(\mathbf{b})$, the integration on the impact parameter can be done exactly leading to

$$\begin{aligned} \sigma_{hA} &= 2\pi R_A^2 \left[\kappa_h - \frac{1}{4}\kappa_h^2 + \cdots + (-1)^{n-1}\frac{\kappa_h^n}{nn!} + \cdots\right] \\ &= 2\pi R_A^2 \left[\gamma + \ln \kappa_h + E_1(\kappa_h)\right] \ , \end{aligned} \tag{3}$$

where $\kappa_h = A\sigma_{hN}/(2\pi R_A^2)$, $\gamma = 0.5772$ is Euler's constant and $E_n(x)$ is the exponential integral function of rank n. The dimensionless quantity κ_h serves as an impact parameter averaged effective number of scatterings. For small value of κ_h, $\sigma_{hA} \to 2\pi R_A^2 \kappa_h = A\sigma_{hN}$, the total hA cross section is proportional to A. In the limit $\kappa_h \to \infty$, the destructive interference between multiple scattering amplitudes reduces the cross section, $\sigma_{hA} \to 2\pi R_A^2(\gamma + \ln \kappa_h)$. Namely, the effective number of scatterings is large and the total cross section approaches the geometric limit $2\pi R_A^2$, a surface term which varies roughly as $A^{2/3}$. In the kinematical region that we are interested in none of these limits are actually approached. The shadowing effect is determined by the strength of κ_h, which is different for a $h = q\bar{q}$ than for a $h = gg$ case.

In the Glauber eikonal approximation, the total cross section $\sigma(\gamma^\star A)$ is given by

$$\sigma(\gamma^\star A) = \int d^2b \int_0^1 dz \int d^2\mathbf{r} |\psi(z, \mathbf{r})|^2 2(1 - e^{-\sigma_{q\bar{q}N}(\mathbf{r},z) T_A(b)/2}), \tag{4}$$

where

$$|\psi(z, \mathbf{r})|^2 = \frac{6\alpha_{\rm em}}{(2\pi)^2} \sum_1^{N_f} e_i^2 P(z) a^2 K_1(a\mathbf{r})^2 \to \frac{6\alpha_{\rm em}}{(2\pi)^2} \sum_1^{N_f} e_i^2 \frac{1}{\mathbf{r^2}} , \tag{5}$$

is the photon wave function, $\sigma_{q\bar{q}N}$ is given by (6), z is the fraction of the energy carried by the quark (antiquark), b is the impact parameter and $T_A(b)$ is the nuclear thickness function. The nuclear cross section is therefore reduced when compared to the simple addition of free nucleon cross sections.

For a given Q^2, all $q\bar{q}$ configurations with the separation size $r_t^2 > 1/Q^2$ are possible, but the virtual photon wavefunction $|\psi_{\gamma^*}| \sim 1/r_t^4$ favors the smallest value of $r_t^2 \simeq 1/Q^2$ where the cross section is small and no significant shadowing is expected. The solution to this problem comes from the fact that the nucleon structure function exhibits a strong scaling violation in the small x region at the moderate (semihard) momentum transfer $0.8\ \text{GeV}^2 < Q^2 < Q^2_{\rm SH}$ where $Q^2_{\rm SH} \simeq 3\ \text{GeV}^2$. As we show, the strong scaling violation in this region can be understood in the context of perturbative QCD. The gluon density grows rapidly with $1/r_t^2$ in the small x region, which can compensate the inherent "smallness" of the cross sections of "hard" QCD processes. As a consequence, the semihard processes can compete successfully with the "soft" processes as described in the VMD model and continue to provide the shadowing mechanism up to some moderately high value of $Q^2 \sim Q^2_{\rm SH}$. In terms of the anomalous dimension, $\gamma(Q^2) = d \ln xg_N / d \ln Q^2$, the cross section in (6) can be written as

$$\sigma_{q\bar{q}N} \propto \frac{(Q^2)^\gamma}{Q^2} . \tag{6}$$

At large Q^2, the anomalous dimension becomes greater than 1 and it delays the rapid decrease of the cross section due to the "smallness" of the configuration size, as first argued by Gribov, Levin and Ryskin in [5]. We refer to this as the perturbative shadowing mechanism as it can be computed in perturbative QCD. At even higher values of Q^2, $Q^2 > Q^2_{\rm SH}$, the scaling violation becomes weak (logarithmic), and the perturbative shadowing mechanism ceases to be effective. In this case, both the nucleon and the nuclear structure function evolve slowly at the same rate. The shadowing ratio developed by both perturbative and non-perturbative mechanisms in the relatively low-Q^2 region persists in the high Q^2 region but tends to 1 rather slowly as $Q^2 \to \infty$.

In contrast to the VMD model, the x-dependent cross section $\sigma_{q\bar{q}N}$ predicts an additional x-dependence of the shadowing ratio apart from the coherence length dependence in the perturbative region. As a result, one does not in general expects a saturation of the shadowing ratio as x decreases below the coherence limit $x < 10^{-2}$. On the other hand, as Q^2 decreases, the gluon distribution changes from a singular small-x behavior (hard pomeron regime) to the less singular one (soft pomeron regime). The shadowing ratio becomes flatter as Q^2 decreases. The observed saturation of the shadowing ratio in the small-x region [2] is thus a non-perturbative, low-Q^2 feature.

Similarly, the nuclear gluon density can be studied by considering a deeply-inelastic scattering of a virtual colorless probe (e.g. the virtual "Higgs boson") with the nucleus where the interaction proceeds via a gluon pair gg component of the virtual probe. This has been considered by Mueller [11] and recently by Ayala F, Gay Ducati and Levin (AGL) [12]. In contrast to the quark distribution, the gluon structure functions for both a nucleon and a nucleus are poorly known, especially in the small-x regime though they are of extreme importance for the semihard QCD processes at high energies. Most of our knowledge on the gluon distribution comes from the theoretical expectations based on perturbative QCD constrained by the scaling violation of F_2^N and the prompt photon experiments [17]. The nuclear gluon density may also be studied in the Glauber multiple scattering model where $\sigma_{q\bar{q}N}$ in (6) is to be replaced by σ_{ggN}. Simple color group representation argument relates these two cross sections by $\sigma_{ggN} = 9\sigma_{q\bar{q}N}/4$. However, what makes the gluon case very different from the quark case is the unknown initial (non-perturbative) gluon density in the nucleus. There is very little experimental information on the gluon shadowing at low Q^2 and small x. The VMD model is not applicable here since the low-lying meson spectroscopy for gg-like states is poorly known. This would make this approach very uncertain in predicting the amount of gluon shadowing in the nucleus.

However, the large σ_{ggN} implies an even stronger scaling violation of gluon density than in the case of quarks making the perturbative shadowing a dominant mechanism. As a consequence, the shadowing ratio is largely determined by the perturbative calculation at $Q^2 = Q^2_{\rm SH}$. That is, the large anomalous dimension of gluon distribution function for a nucleon drives the shadowing ratio rapidly to approach the perturbative value at moderately large Q^2, $Q^2 = Q^2_{\rm SH}$, and the initial shadowing (at low Q^2) becomes relatively unimportant. For $Q^2 > Q^2_{\rm SH}$, the scaling violation becomes weaker and the shadowing ratio determined by the perturbative shadowing mechanism at the semihard scale persists and evolves slowly. The x-dependence of the shadowing ratio can be also predicted to be non-saturating, a generic feature of the perturbative shadowing. We therefore suggest that the nuclear gluon shadowing at $Q^2 > Q^2_{\rm SH} \simeq 3$ GeV^2 and at small x can be predicted in the context of perturbative QCD. The prediction is based on the scaling violation of the gluon structure function and the existence of the perturbative shadowing in the Glauber multiple scattering model.

At small x, the structure function of a nucleus can be written in terms of the virtual photon-nucleus cross section

$$F_2^A(x, Q^2) = \sum_i e_i^2 x f_A(x, Q^2) = \frac{Q^2}{4\pi^2 \alpha_{\rm em}} \sigma(\gamma^* A) \ , \tag{7}$$

where $xf_A(x, Q^2)$ is the (sea) quark distribution function. Using (12) and substituting integration over $(z, \mathbf{r_t})$ to (x', Q'^2) in (9), one obtains for (sea)quarks [15]

$$xf_A(x, Q^2) \;=\; xf_A(x, Q_0^2) + \frac{3R_A^2}{8\pi^2} x \int_x^1 \frac{dx'}{x'^2} \int_{Q_0^2}^{Q^2} dQ'^2 \left[\gamma + \ln(\kappa_q) + E_1(\kappa_q)\right] \;, \tag{8}$$

where the effective number of scatterings κ_q is given

$$\kappa_q(x, Q^2) = \frac{2A\pi}{3R_A^2 Q^2} \alpha_s(Q^2) x g_N^{\rm DLA}(x, Q^2) \;, \tag{9}$$

Expanding $[\cdots]$ and keeping only the first term which is proportional to κ_q, one recovers the result for the nucleon in the same DLA approximation. We find our result for $F_2^N(x, Q^2)$ to be in excellent agreement with the recent HERA data for a broad range of x and Q^2 (see Figs. 2 and 3 in Ref. 15).

In principle, the initial condition $xf_A(x, Q_0^2)$ in (8) may be calculated in the vector-meson-dominance (VMD) model. Fortunately, there have been some experimental measurements on the nuclear quark shadowing in the low-Q^2 region so that the initial condition can be expressed in terms of the production of the initial nucleon structure function and the shadowing ratio $R_0^q(x)$

$$F_2^A(x, Q_0^2) = AR_0^q(x) F_2^N(x, Q_0^2) \;, \tag{10}$$

where $F_2^N(x, Q_0^2)$ is nucleon structure function. Recently E665 Collaboration has measured the nuclear shadowing effect in muon scatterings off ^{40}Ca and ^{208}Pb at low x [2]. In general, the small x data are measured at low Q^2, e.g., for $x = 6 \times 10^{-4}$ the average $\langle Q^2 \rangle = 0.26$ GeV^2 while $x = 6 \times 10^{-3}$ corresponds to $\langle Q^2 \rangle = 1.35$ GeV^2. We parametrize the initial shadowing ratio $R_0^q(x)$ at $Q_0^2 = 0.4$ GeV^2 and we calculate the nuclear structure function at the measured $\langle Q^2 \rangle$ values at different x values. The nuclear shadowing ratio is defined by

$$\begin{aligned} R_q(x, Q^2) \;&=\; \frac{F_2^A(x, Q^2)}{AF_2^N(x, Q^2)} \\ &=\; \frac{R_q^0(x) F_2^N(x, Q_0^2) + \Delta F_2^A(x; Q^2, Q_0^2)}{F_2^N(x, Q_0^2) + \Delta F_2^N(x; Q^2, Q_0^2)} \;, \end{aligned} \tag{11}$$

where $\Delta F_2 \equiv F_2 - F_2(Q_0^2)$ can be explicitly calculated by performing the double integration over x' and Q'^2 in (8). The results for ^{40}Ca and ^{208}Pb are shown in Fig. 2.

The x-dependence of nuclear quark shadowing ratio $R_q = F_2^A/(AF_2^N)$ at various Q^2 for ^{208}Pb and ^{40}Ca. The lower panels represent the parameterizations of initial shadowing ratios evolved to the experimental $\langle Q^2 \rangle_{\rm exp}$ values. The non-saturation of $R_q(x)$ as x decreases at large Q^2 is the feature of the perturbative shadowing mechanism.

The lower panels of Fig. 2 show our parametrizations of initial shadowing ratio at Q_0^2 evolved to the measured $\langle Q^2 \rangle$ compared to the experimental data from E665. For $\langle Q^2 \rangle < Q_0^2$, we take it to be at the minimal scale Q_0^2. As is evident from the comparison, our parametrizations faithfully represent the experimental data at small x. The shadowing ratio, $R_q(x, Q^2)$, at high values of Q^2 are shown in the upper panels of Fig. 2.

We note that at large Q^2 the nuclear shadowing effect is reduced but does not diminish, i.e. it is not a higher twist effect. This can be understood as the interplay between the

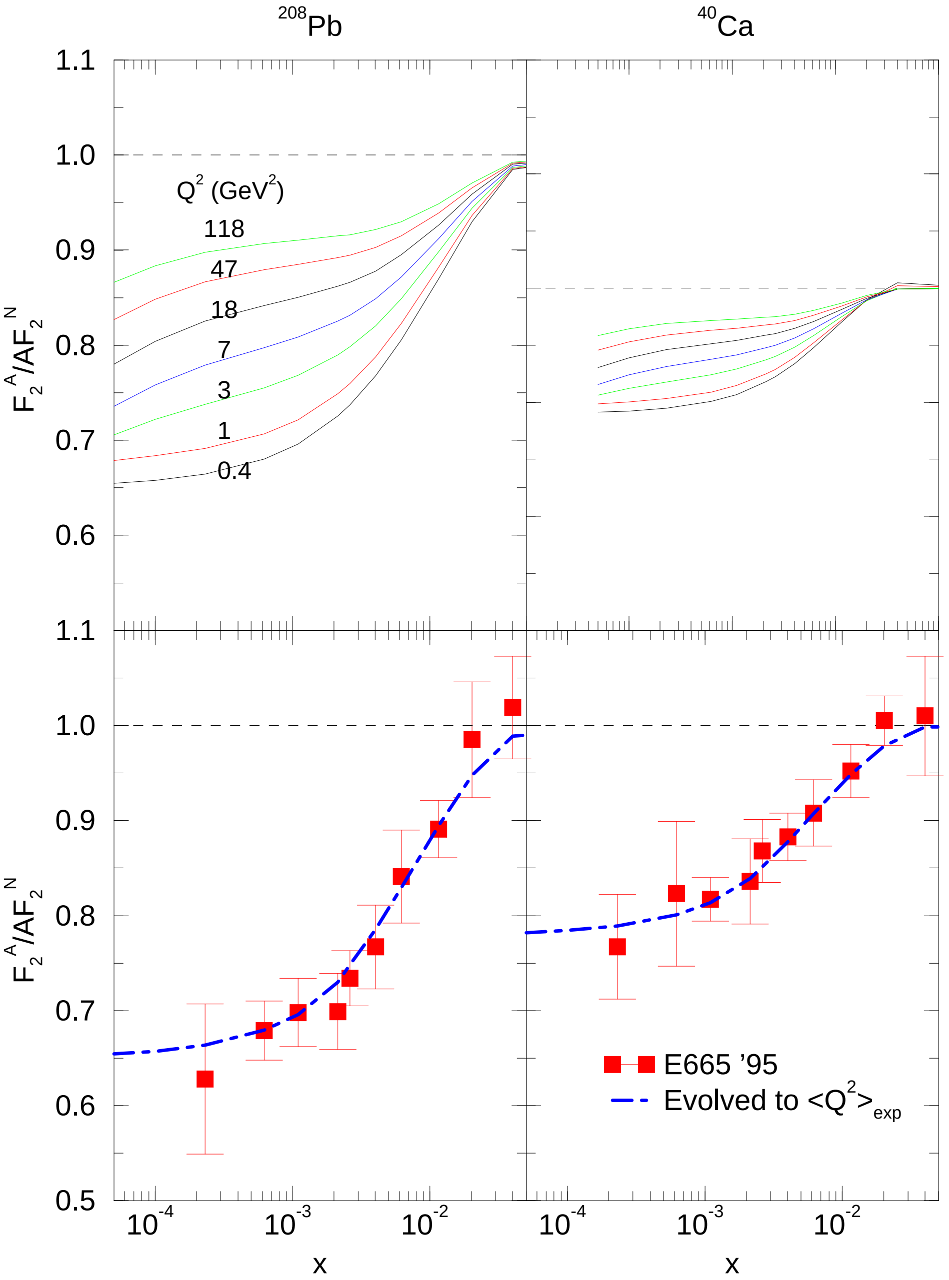

Figure 1:

perturbative and the non-perturbative shadowing mechanisms. The nuclear quark density is initially shadowed by R_q^0 at Q_0^2 compared to the free nucleon case due to some non-perturbative mechanism such as coherent scatterings of the ρ-meson as discussed in the VMD model [14]. As Q^2 increases from Q_0^2, the nucleon structure function increases by $\Delta F_2^N(x; Q^2, Q_0^2)$ as governed by the GLAP evolution equation in the DLA. If the nuclear F_2^A increases by the same amount (times A), i.e., we neglect the multiple scattering effect and evolve it according to the same GLAP equation, the initial shadowing effect in (11) decreases quickly due to the strong scaling violation at low Q^2 ($\Delta F_2^N(x; Q^2, Q_0^2)$ is not small compared to $F_2^N(x, Q_0^2)$). This is illustrated in Fig.5 in Ref. 15 where the shadowing ratio is calculated by taking the first term in the expansion $[\cdots]$ in (8) and plotted as function of Q^2 at a fixed $x = 10^{-4}$. The shadowing effect disappears quickly when both the nucleon and nuclear structure functions evolve according to the GLAP equation. Also plotted in Fig. 5 in Ref. 15 is the double scattering case where we take the first two terms in the expansion

$$[\gamma + \ln \kappa_q + E_1(\kappa_q)] \simeq \kappa_q - \frac{1}{4}\kappa_q^2 \, . \tag{12}$$

As it is evident from Fig. 5 in Ref. 15, the double scattering overestimates the amount of shadowing. Nevertheless, it accounts for most of the multiple scattering effect.

The interplay between soft physics and the partonic picture of the nuclear shadowing is also evident in the x-dependence of R_q in Fig. 4. in Ref. 15. The apparent flatness of the shadowing ratio at low Q^2 in the small-x region is altered by the perturbative evolution. This is due to the singular behavior of $xg_N^{\rm DLA}$ as $x \to 0$ at large Q^2 leading to the strong x-dependence of the effective number of scatterings, $\kappa_q(x)$. Thus, the saturation of the R_q as x decreases is a feature only at low Q^2, $Q^2 < 2$ GeV^2 where the gluon density is not so singular, and we do not expect the saturation to happen for higher values of Q^2.

In the previous section, we emphasized the importance of the interplay between the non-perturbative and perturbative shadowing mechanisms in order to predict the nuclear quark shadowing at large Q^2. In principle, the prediction for the nuclear gluon shadowing could be uncertain because there is no experimental information on the gluon shadowing at low Q^2. However, as we demonstrate below that this is not the case and the gluon shadowing can be unambiguously predicted for large Q^2 in the context of perturbative QCD.

The gluon distribution in a nucleus can be calculated in the Glauber model similarly to the quarks [12]

$$xg_A(x,Q^2) \;=\; xg_A(x,Q_0^2) + \frac{2R_A^2}{\pi^2}\int_x^1 \frac{dx'}{x'}\int_{Q_0^2}^{Q^2} dQ'^2\,[\gamma + \ln(\kappa_g\tau) + E_1(\kappa_g\tau)] \;, \tag{13}$$

The essential difference between the quark and gluon cases is different splitting functions and the effective number of scatterings, $\kappa_g = 9\kappa_q/4$ due to different color representations that the quark and the gluon belong to. These two effects combined result in the 12 times faster increase of the gluon density with Q^2 than in the case of the sea quarks in the region of small x. The two important effects which make the gluon shadowing quite different from the quark shadowing are the stronger scaling violation in the semihard scale region and a larger perturbative shadowing effect. This can be seen by considering the shadowing ratio

$$\begin{aligned} R_g(x,Q^2) &= \frac{xg_A(x,Q^2)}{Axg_N(x,Q^2)} \\ &= \frac{xg_N(x,Q_0^2)R_g^0(x) + \Delta xg_A(x;Q^2,Q_0^2)}{xg_N(x,Q_0^2) + \Delta xg_N(x;Q^2,Q_0^2)} \;, \end{aligned} \tag{14}$$

where $R_g^0(x)$ is the initial shadowing ratio at Q_0^2 and $\Delta xg(x;Q^2,Q_0^2)$ is the change of the gluon distribution as the scale changes from Q_0^2 to Q^2. The strong scaling violation due to a larger κ_g at small x causes $\Delta xg_N(x;Q^2,Q_0^2) \gg xg_N(x,Q_0^2)$ as Q^2 is greater than $1 \sim 2$ GeV^2. The dependence of $R_g(x,Q^2)$ on the initial condition $R_g^0(x)$ diminishes and the perturbative

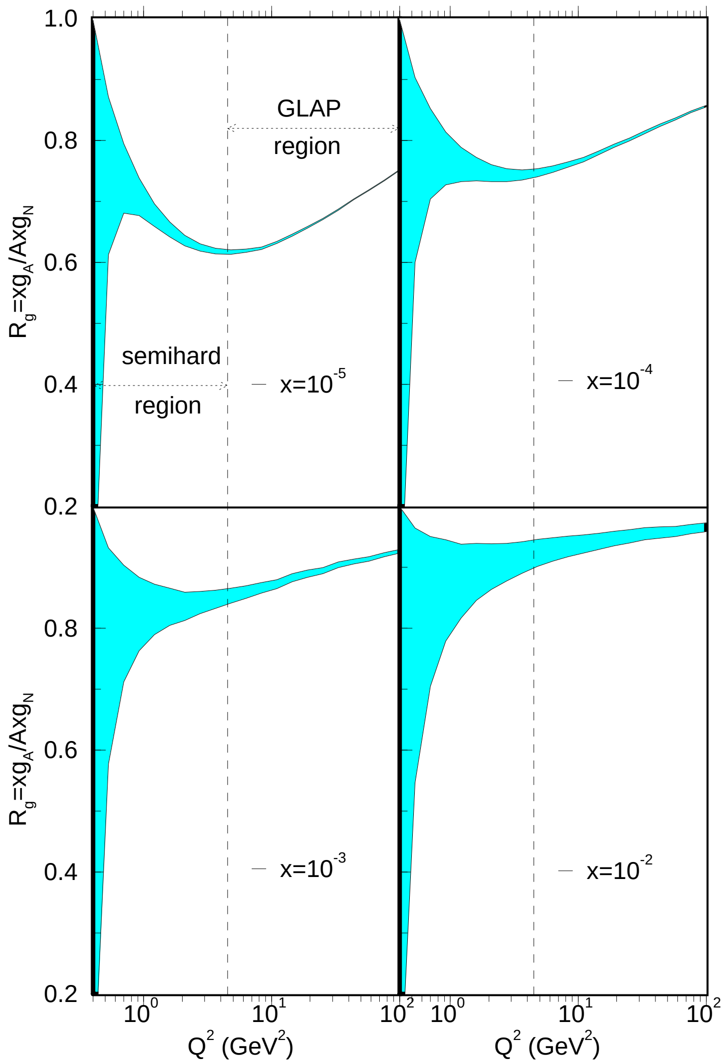

Figure 2: The x-dependence of the gluon shadowing ratio at various Q^2 values. The shaded region indicates the uncertainty due to the initial conditions.

shadowing mechanism takes over, i.e.

$$R_g(x,Q^2) \to \frac{\Delta x g_A(x;Q^2,Q_0^2)}{\Delta x g_N(x;Q^2,Q_0^2)}\,, \tag{15}$$

for $Q^2 > 2$ GeV^2. This can be seen in Fig. 3.

The above statement can be made more rigorous by taking a partial derivative of (14) with respect to $\ln Q^2$ at a fixed x

$$\frac{\partial R_g(x,Q^2)}{\partial \ln Q^2} = \gamma(Q^2)\left[R_g^{\rm PT}(x,Q^2) - R_g(x,Q^2)\right]\,, \tag{16}$$

where the anomalous dimension $\gamma(Q^2)$ and the so-called perturbative shadowing ratio $R_g^{\rm PT}$ are defined

$$\gamma(Q^2) \quad = \quad \frac{\partial \ln x g_N(x,Q^2)}{\partial \ln Q^2}$$

$$R_g^{\rm PT} \quad = \quad \frac{\partial x g_A(x,Q^2)/\partial \ln Q^2}{A \partial x g_N(x,Q^2)/\partial \ln Q^2} \ . \tag{17}$$

Note that $R_g^{\rm PT}$ is the ratio of the derivative of xg_A to that of xg_N, which is independent of the initial shadowing ratio and can be calculated perturbatively. In the small-x,

$$R_g^{\rm PT} \simeq \frac{\gamma + \ln\kappa_g + E_1(\kappa_g)}{\kappa_g} = 1 - \frac{\kappa_g}{4} + \frac{\kappa_g^2}{18} - \cdots \ . \tag{18}$$

The interesting feature of (16) is the negative sign in front of R_g on the right hand side such that it is self-stabilizing. If $R_g < R_g^{\rm PT}$ at Q^2 and $\partial R_g/\partial \ln Q^2 > 0$, the shadowing ratio increases with Q^2; while for $R_g < R_g^{\rm PT}$, the shadowing ratio decreases with Q^2. As a result, the Q^2-evolution of R_g is such that it is always in the process of approaching $R_g^{\rm PT}$. Because $R_g^{\rm PT}$ also changes with Q^2, the Q^2-evolution of R_g never stops. The anomalous dimension $\gamma(Q^2)$ determines how fast R_g is approaching $R_g^{\rm PT}$. Introduce an important scale $Q^2_{\rm SH} = 3$ GeV^2 ("SH" stands for "semihard") where $\gamma(Q^2_{\rm SH}) \simeq$O(1). In the semihard region $Q_0^2 < Q^2 < Q^2_{\rm SH}$, $\gamma(Q^2)$ is large and R_g approaches $R_g^{\rm PT}(Q^2_{\rm SH})$ fast regardless of what the initial shadowing one has to set at Q_0^2. It is precisely in this region that κ_g is large and (18) gives a large shadowing correction. As $Q^2 > Q^2_{\rm SH}$, the anomalous dimension $\gamma(Q^2)$ gets small and $R_g^{\rm PT}$ approaches 1 fast and the shadowing ratio R_g evolves slowly. Thus, the behavior of the Q^2-evolution of the gluon shadowing can be understood by the interplay between the anomalous dimension of the nucleon gluon structure function and the perturbative shadowing mechanism.

Approximating the perturbative shadowing by $R_g^{\rm PT} = R_g^{\rm PT}(Q^2_{\rm SH})$ for $Q_0^2 < Q^2 < Q^2_{\rm SH}$ and $R_g^{\rm PT} = 1$ for $Q^2 > Q^2_{\rm SH}$, one obtains the shadowing ratio for $Q^2 > Q^2_{\rm SH}$

$$R_g(t) = 1 - \left[1 - R_g^{\rm PT}(t_{\rm SH})\right] e^{-\int_{t_{\rm SH}}^{t} \gamma(t')dt'} \ . \tag{19}$$

The evolution factor $\exp[-\int]$ no longer falls rapidly and R_g evolves rather slowly. Thus, the Q^2-behavior of gluon shadowing at large Q^2 can be roughly described by an initial condition at $Q^2_{\rm SH}$ followed by a GLAP evolution. The important point is that the initial condition at $Q^2 = Q^2$SH is pre-determined by the perturbative shadowing. Our main conclusion is that even though $R_g^{\rm PT}(Q^2)$ approaches 1 quickly as Q^2 increases beyond $Q^2_{\rm SH}$ (a higher twist effect), the shadowing ratio at large Q^2 is still governed by the perturbative shadowing at the *semihard scale*, namely $R_g^{\rm PT}(Q^2_{\rm SH})$.

The x-dependence of the gluon shadowing can also be predicted as long as $Q^2 > Q^2_{\rm SH}$ where the influence of the initial condition is minimal. Fig. 3 in Ref. 15 shows the x-dependence of the gluon shadowing ratio at various Q^2 values. The shaded region is bounded by the distributions calculated using two drastically different initial conditions $R_g^0 = 0$ and $R_g^0(x) = 1$. It is clear that the shape of the distribution is quite robust in the small-x region regardless of what initial conditions one may choose. Due to the perturbative nature of the shadowing, these distributions do not exhibit a saturation as x decreases. This is related to the singular behavior of the nucleon gluon distribution at large Q^2 and small x. As long as the nucleon gluon density does not saturates at small x, the shadowing ratio does not saturate either. This is in accordance with the observation by Eskola, Qiu and Wang [7] in the context of the gluon recombination model. The rapid Q^2-evolution of the gluon shadowing ratio in the low Q^2 region found by Eskola [23] can be understood in our approach as the quick approach of the initial shadowing ratio to its perturbative value (see Fig. 7 in Ref. 15). In Eskola's approach some shadowing persists even at $Q^2 = 100$ GeV^2 which can also be understood in our picture as the region of fully developed GLAP evolution. We note that multiple scatterings inside the nucleon are also possible in the region of very small x, where the eikonalization of the nucleon cross section is needed. However, in this region, the DLA breaks down and a BFKL resummation is necessary.

So far we have confined ourselves to the impact parameter averaged nuclear structure function. However, in the binary approximation of hard scattering processes in pA and AA collisions, one has to calculate the parton cross section at the nucleon-nucleon level at each impact parameter. In addition, to enhance the possible signal of a quark-gluon plasma in heavy-ion collisions, one triggers on central events where the impact parameter is small (e.g. $b < 2$ fm). It is thus necessary to study the impact parameter dependence of the nuclear shadowing effect.

Intuitively, one expects that the nuclear shadowing effect should depend on the local nuclear thickness at a given impact parameter. In the Glauber approach, the effective number of scatterings is a product of the cross section and the nuclear thickness function. Since the shadowing is a non-linear effect in the effective number of scatterings, the impact parameter dependent shadowing ratio cannot be factorized into a product of an average shadowing ratio and the nuclear thickness function, as has been done in previous works [24].

The impact parameter dependent nuclear structure function $x\tilde{g}_A(x, Q^2; \mathbf{b})$ is defined as

$$xg_A(x, Q^2) = \int d^2\mathbf{b}\, x\tilde{g}_A(x, Q^2; \mathbf{b}) \ . \tag{20}$$

where

$$\begin{aligned} x\tilde{g}_A(x, Q^2; \mathbf{b}) &= x\tilde{g}_A(x, Q_0^2; \mathbf{b}) + \frac{4}{\pi^3} \int_x^1 \frac{dx'}{x'} \int_{Q_0^2}^{Q^2} dQ'^2 \\ & \quad 2\left[1 - e^{-\sigma_{ggN} T_A(\mathbf{b})/2}\right] \ , \end{aligned} \tag{21}$$

and $x\tilde{g}_A(x, Q_0^2; \mathbf{b})$ is the initial condition at a fixed impact parameter $\mathbf{b}$. As shown in the previous section, the prediction for gluon shadowing ratio at $Q^2 > 3$GeV^2 does not depend on the initial condition. Thus, as an illustration we take the initial shadowing ratio to be 1 for all $\mathbf{b}$'s. The impact parameter dependent shadowing ratio,

$$R_g(x, Q^2; \mathbf{b}) = \frac{x\tilde{g}_A(x, Q^2; \mathbf{b})}{T_A(\mathbf{b}) x g_N(x, Q^2)} \ . \tag{22}$$

is plotted in Fig. 4.

In summary, the nuclear shadowing phenomenon is a consequence of the parton coherent multiple scatterings. While the quark density shadowing arises from an interplay between "soft" physics and the semihard QCD process, the gluon shadowing is largely driven by a perturbative shadowing mechanism due to the strong scaling violation in the small-x region. The gluon shadowing is thus a robust phenomenon at large Q^2 and can be unambiguously predicted by perturbative QCD.

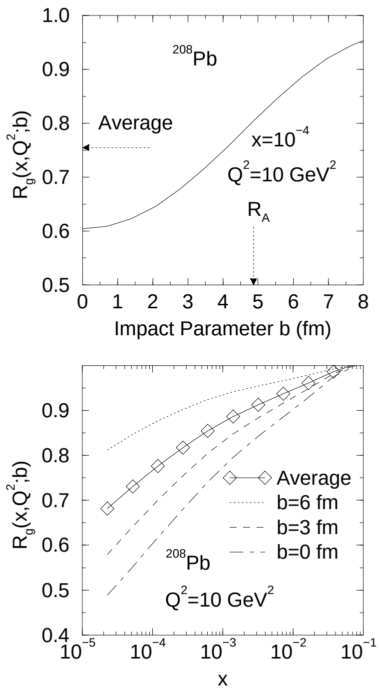

Figure 3: The impact parameter dependent gluon shadowing calculated assuming $R_g^0 = 1$ for any b. The upper panel is the shadowing ratio as function of b at fixed values of $x = 10^{-4}$ and $Q^2 = 10$ GeV^2. Tle lower panel shows the x-dependence of the shadowing ratio at a fixed $Q^2 = 10$ GeV^2 and various values of b.

The scale dependence of the nucleon structure function was used to put a stringent constraint on the gluon density inside the nucleon in the double logarithm approximation. It is shown that the strong scaling violation of the nucleon structure function in the semihard momentum transfer region $0.8 < Q^2 < 3$ GeV^2 at small x can be reliably described by perturbative QCD and is a central key to the understanding of the scale dependence of the nuclear shadowing effect.

The impact parameter dependence of gluon shadowing is a non-linear effect in the nuclear thickness function. It is important to correctly incorporate the impact parameter dependence of the nuclear structure function when one calculates the QCD processes in the central nucleus collisions.

Future Plans: We plan to re-examine hard processes which are sensitive to the gluon density in a nucleus at small x, such as minijet production and direct photon production at RHIC and LHC energies.

References

[1] NMC Collaboration, P. Amaudruz *et al.*, Z. Phys. C **51**, 387 (1991); Z. Phys.C **53**, 73 (1992); Phys. Lett. B **295**, 195 (1992); NMC Collaboration, M. Arneodo *et al.*, Nucl. Phys. B **441**, 12 (1995).

[2] E665 Collaboration, M.R. Adams *et al.*, Phys. Rev. Lett. **68**, 3266 (1992); Phys.

Lett. B **287**, 375 (1992); Z. Phys. C **67**, 403 (1995).

[3] D. Alde *et al.*, Phys. Rev. Lett. **66**, 133 (1991).

[4] S. Gavin and J. Milana, Phys. Rev. Lett. **68**, 1834; C.J. Benesh, J. Qiu and J.P. Vary, Phys. Rev. C **50**, 1015 (1994).

[5] L.V. Gribov, E.M. Levin and M.G. Ryskin, Phys. Rep. **100**, 1 (1983); E. Laenen and E. Levin, Nucl. Phys. B **451**, 207 (1995).

[6] A.H. Mueller and J. Qiu, Nucl. Phys. B **268**, 427 (1986); J. Qiu, Nucl. Phys. B **291**, 746 (1987).

[7] K.J. Eskola, J. Qiu and X.-N. Wang, Phys. Rev. Lett. **72**, 36 (1994).

[8] L. Frankfurt and M. Strikman, Nucl. Phys. B **316**, 340 (1989); L. Frankfurt, M. Strikman and S. Liuti, Phys. Rev. Lett. **65**, 1725 (1990).

[9] S.J. Brodsky and H.J. Lu, Phys. Rev. Lett. **64**, 1342 (1990).

[10] N.N. Nikolaev, Z. Phys. C **32**, 537 (1986); N.N. Nikolaev and B.G. Zakharov, Phys. Lett. B **260**, 414 (1991); Z. Phys. C **49**, 607 (1991).

[11] A.H. Mueller, Nucl. Phys. B **335**, 115 (1990).

[12] A.L. Ayala F, M.B. Gay Ducati and E.M. Levin, Nucl. Phys. B **493**, 305 (1997).

[13] V.N. Gribov and L.N. Lipatov, Sov. J. Nucl. Phys. **15**, 438 (1972); G. Altarelli and G. Parisi, Nucl. Phys. B **126**, 298 (1977); Yu.L. Dokshitser, Sov. Phys. JETP **46**, 641 (1977).

[14] see e.g., G. Piller, W. Ratzka and W. Weise, Z. Phys. A **352**, 427 (1995); T.H. Bauer, R.D. Spital and D.R. Yennie and F.M. Pipkin, Rev. Mod. Phys. **50**, 261 (1978).

[15] Z. Huang, H. J. Lu and I. Sarcevic. AZPH-TH-97-07, hep-ph/9705250, submitted to Nucl. Phys. **A**

[16] R.J. Glauber, in *Lectures in theoretical physics*, ed. W.E. Brittin *et al.* (Interscience Publishers, New York, 1959); R.J. Glauber and G. Matthiae, Nucl. Phys. B **21**, 135 (1970).

[17] A.D. Martin, R.G. Roberts and W.J. Stirling, Phys. Lett. B **387**, 419 (1996); H.L. Lai, J. Huston, S. Kuhlmann, F. Olness, J. Owens, D. Soper, W.K. Tung and H. Weerts, Phys. Rev. D **55**, 1280 (1997); M. Glueck, E. Reya and A. Vogt, Z. Phys. C **67**, 433 (1995).

[18] E.A. Kuraev, L.N. Lipatov and V.S. Fadin, Sov. Phys. JETP **45**, 199 (1977); Ya.Ya. Balitskii and L.V. Lipatov, Sov. J. Nucl. Phys. **28**, 822 (1978); L.N. Lipatov, Sov. Phys. JETP **63**, 904 (1986).

[19] L. McLerran and R. Venugopalan, Phys. Rev. D **49**, 2233 (1994); A. Kovner, L. McLerran and H. Weigert, Phys. Rev. D **52**, 6231 (1995); D **52**, 3809 (1995).

[20] A.J. Brodsky and A.H. Mueller, Phys. Lett. B **206**, 685 (1988); G. Farrar, L. Frankfurt, M. Strikman and H. Liu, Phys. Rev. Lett. **64**, 1996 (1990).

[21] B. Blattel, G. Baym, L. Frankfurt and M. Strikman, Phys. Rev. Lett. **70**, 896 (1993); L. Frankfurt, G. Miller and M. Strikman, Phys. Lett. B **304**, 1 (1993).

[22] B. Kopeliovich and B. Povh, Phys. Lett. B **367**, 329 (1996).

[23] K.J. Eskola, Nucl. Phys. B **400**, 240 (1993).

[24] K.J. Eskola, Z. Phys. C **51**, 633 (1991).